

Nonunitary Triplet Pairing in the Centrosymmetric Superconductor LaNiGa_2

A. D. Hillier,¹ J. Quintanilla,^{1,2} B. Mazidian,^{1,3} J. F. Annett,³ and R. Cywinski⁴

¹*ISIS Facility, STFC Rutherford Appleton Laboratory, Harwell Science and Innovation Campus, Oxfordshire, OX11 0QX, United Kingdom*

²*SEPnet and Hubbard Theory Consortium, School of Physical Sciences, University of Kent, Canterbury, CT2 7NH, United Kingdom*

³*H. H. Wills Physics Laboratory, University of Bristol, Tyndall Avenue, Bristol, BS8 1TL, United Kingdom*

⁴*School of Applied Sciences, University of Huddersfield, Queensgate, Huddersfield, HD1 3DH, United Kingdom*

(Received 9 January 2012; published 27 August 2012)

Muon spin rotation and relaxation experiments on the centrosymmetric intermetallic superconductor LaNiGa_2 are reported. The appearance of spontaneous magnetic fields coincides with the onset of superconductivity, implying that the superconducting state breaks time reversal symmetry, similarly to noncentrosymmetric LaNiC_2 . Only four triplet states are compatible with this observation, all of which are nonunitary triplets. This suggests that LaNiGa_2 is the centrosymmetric analogue of LaNiC_2 . We argue that these materials are representatives of a new family of paramagnetic nonunitary superconductors.

DOI: [10.1103/PhysRevLett.109.097001](https://doi.org/10.1103/PhysRevLett.109.097001)

PACS numbers: 74.20.Rp, 74.25.Ha, 74.70.Dd, 76.75.+i

Symmetry breaking is a central concept of physics for which superconductivity provides one of the best understood paradigms. In a conventional superconductor [1] gauge symmetry is broken, while unconventional superfluids and superconductors break other symmetries as well [2]. Examples include ^3He [3], cuprate high-temperature superconductors [4], the ruthenate Sr_2RuO_4 [5], and, more recently, noncentrosymmetric LaNiC_2 [6]. The latter has weak spin-orbit coupling (SOC) [7], low symmetry, and is a nonunitary superconductor. In a nonunitary superconductor the pairing states of the spin-up and spin-down Fermi surfaces are different. At the instability, a spin-up superfluid can coexist with spin-down Fermi liquid. While nonunitary triplet superconductivity is well-established in ferromagnetic superconductors [8], its occurrence in paramagnetic LaNiC_2 remains puzzling. Here we provide experimental evidence of this phenomenon in another, compositionally related, but centrosymmetric superconductor: LaNiGa_2 . We also advance an explanation in terms of a coupling between triplet instabilities and paramagnetism that is quite generic and for which these two could provide the first examples of what might be a larger class of materials.

In general, unconventional pairing can be difficult to establish in any given material. However, evidence for time-reversal symmetry (TRS) breaking in particular can be shown through the detection of spontaneous but very small internal fields [2]. Muon spin relaxation and rotation (μSR) is especially sensitive for detecting small changes in internal fields and can easily measure fields of 0.1 G which corresponds to $\approx 0.01\mu_B$. This makes μSR an extremely powerful technique for measuring the effects of TRS breaking in exotic superconductors. Direct observation of TRS breaking states is extremely rare and spontaneous fields have been observed in this way only in a few systems: $\text{PrOs}_4\text{Sb}_{12}$ [9], Sr_2RuO_4 [10] (where TRS breaking

was subsequently confirmed by optical measurements [11]), B phase of UPt_3 [12] (although not without controversy [13,14]), $(\text{U}, \text{Th})\text{Be}_{13}$ [15], and more recently LaNiC_2 [6], $\text{PrPt}_4\text{Ge}_{12}$ [16], and $(\text{PrLa})(\text{OsRu})_4\text{Sb}_{12}$ [17]. For examples of other systems where the effect is *not* observed, see Refs. [18–21]. Broken TRS in superconductors is especially interesting, because it implies not just unconventional pairing, but the existence of twofold or higher degeneracy of the superconducting order parameter space [22].

The observation of broken TRS in LaNiC_2 was particularly surprising because of the low symmetry of this orthorhombic, noncentrosymmetric, material [6]. Symmetry analysis has shown that the low dimensionality of this structure, with C_{2v} point group, gives rise to only 12 possible gap functions. Of these, only 4 break TRS and these are all nonunitary triplet pairing states [6]. These 4 gap functions are all derived from one-dimensional irreducible representations of the point group, implying that the only possible order parameter degeneracy is derived from the triplet Cooper pair spin orientational degree of freedom. A subsequent analysis of the effects of SOC on this system [7] shows that the SOC always lifts this final degeneracy, leading to a completely nondegenerate order parameter space, which would not be expected to allow spontaneous breaking of TRS at the superconducting transition temperature, T_c [22]. The only way to reconcile this with the experimental observations of broken TRS in this material is to assume that the effect of SOC is weak on the relevant electron states at the Fermi level in this material. Additional experimental evidence for unconventional pairing in LaNiC_2 has been reported recently [23].

In this Letter we report μSR results on the centrosymmetric superconductor LaNiGa_2 showing that TRS is broken on entering the superconducting state. This is a centrosymmetric material, which crystallizes in the

NdNiGa₂ orthorhombic structure, with space group *Cmmm* (*D*_{2h}) [24] (see Fig. 1). Magnetization and heat capacity measurements have previously shown that LaNiGa₂ is a paramagnetic superconductor, with a *T*_c onset of 2.1 K [24]. Heat capacity measurements have shown a specific heat jump $\Delta C/\gamma T_c \approx 1.31$ [25], which is slightly lower than the expected BCS value of 1.43, and the temperature dependence has the conventional BCS exponential form. Specific heat jumps in TRS-breaking superconductors are sometimes lower and sometimes higher than the BCS value, for example Sr₂RuO₄ [26], LaNiC₂ [27], and PrPt₄Ge₁₂ [28], respectively. Below we analyze the possible order parameter symmetries. Although LaNiGa₂ has a different point group to LaNiC₂ and is centrosymmetric, it is similar to LaNiC₂ in that it has only 12 possible superconducting symmetries [4]. For both materials, these are all derived from one-dimensional irreducible representations. In particular, only four of these states break TRS and these are all nonunitary triplet pairing states [see Table I, upper].

The sample was prepared by melting together stoichiometric amounts of the constituent elements in a water-cooled argon arc furnace. The μ SR experiments were carried out using the MuSR spectrometer in longitudinal and transverse geometries. At the ISIS facility, a pulse of muons is produced every 20 ms and has a FWHM of ~ 70 ns. These muons are implanted into the sample and decay with a half-life of 2.2 μ s into a positron which is emitted preferentially in the direction of the muon spin axis and two neutrinos. These positrons are detected and time stamped in the detectors which are positioned either before, F, or after, B, the sample for longitudinal (relaxation) experiments. The forward and backward detectors are each segmented into 32 detectors. Using these counts, the asymmetry in the positron emission can be determined and, therefore, the muon polarization is measured as a function of time. For the transverse field experiments, the magnetic field was applied perpendicular to the initial muon spin direction and momentum. For a more detailed description of the different instrumental geometry can be found in Refs. [29–31].

The sample was powder mounted onto a 99.995 + % pure silver plate. Any muons stopped in silver give a time independent background for longitudinal (relaxation) experiments. The sample holder and sample were mounted

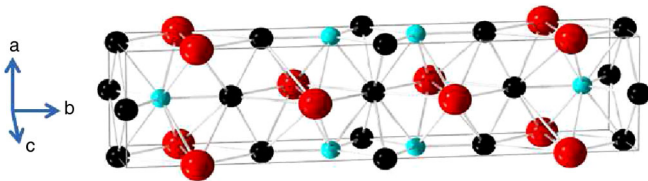


FIG. 1 (color online). The orthorhombic crystal structure of LaNiGa₂. The red spheres (largest) are La, blue spheres (smallest) are Ni, and the black spheres (medium) are Ga.

onto a TBT dilution refrigerator with a temperature range of 0.045–4 K. The stray fields at the sample position are canceled to within 1 μ T by a flux-gate magnetometer and an active compensation system controlling the three pairs of correction coils. The transverse field μ SR experiment was conducted with applied fields between 5 mT and 60 mT, which ensured the sample was in the mixed state. Each field was either applied above the superconducting transition and the sample was then cooled to base temperature [field cooled (FC)] or the sample was first cooled to base temperature and then the field was applied [zero-field cooled (ZFC)]. The sample was cooled to base temperature in zero field and the μ SR spectra were collected upon warming the sample while still in zero field.

The MuSR spectrometer comprises 64 detectors. In software, the data is mapped to two orthogonal virtual detectors each characterized by a phase offset φ . The resulting 2 spectra were simultaneously fitted with a sinusoidal oscillating function with Gaussian relaxation:

$$G_z(t) = \sum_{i=1}^2 A_i \exp\left(-\frac{\sigma_i^2 t^2}{2}\right) \cos(2\pi\nu_i t + \varphi) \quad (1)$$

TABLE I. The upper table shows the gap function of the homogeneous superconducting states allowed by symmetry, for weak spin-orbit coupling. We have used the standard notation $\hat{\Delta}(\mathbf{k}) = \Delta(\mathbf{k})i\hat{\sigma}_y$ for singlet states and $\hat{\Delta}(\mathbf{k}) = i[\mathbf{d}(\mathbf{k}) \cdot \hat{\boldsymbol{\sigma}}]\hat{\sigma}_y$ for triplets, where $\hat{\boldsymbol{\sigma}} \equiv (\hat{\sigma}_x, \hat{\sigma}_y, \hat{\sigma}_z)$ is the vector of Pauli matrices. Here *X*, *Y*, and *Z* are any basis functions in the Brillouin zone of odd parity, such as sink_x , sink_y and sink_z , respectively. Only the four nonunitary triplet states are compatible with our observation of broken TRS. The lower table shows the homogeneous spin-triplet superconducting states allowed by symmetry at *T*_c, for the case of strong spin-orbit coupling. The spin-singlet gap functions are the same as in the weak spin-orbit case. The notation of the possible gap functions is the same as the upper table, except that, here, *A*, *B*, and *C* are (real) constants determined by the microscopic gap equation. Clearly none of these states breaks TRS at *T*_c.

<i>SO</i> (3) × <i>D</i> _{2h}	Gap function (unitary)	Gap function (nonunitary)
¹ A ₁	$\Delta(\mathbf{k}) = 1$...
¹ B ₁	$\Delta(\mathbf{k}) = XY$...
¹ B ₂	$\Delta(\mathbf{k}) = XZ$...
¹ B ₃	$\Delta(\mathbf{k}) = YZ$...
³ A ₁	$\mathbf{d}(\mathbf{k}) = (0, 0, 1)XYZ$	$\mathbf{d}(\mathbf{k}) = (1, i, 0)XYZ$
³ B ₁	$\mathbf{d}(\mathbf{k}) = (0, 0, 1)Z$	$\mathbf{d}(\mathbf{k}) = (1, i, 0)Z$
³ B ₂	$\mathbf{d}(\mathbf{k}) = (0, 0, 1)Y$	$\mathbf{d}(\mathbf{k}) = (1, i, 0)Y$
³ B ₃	$\mathbf{d}(\mathbf{k}) = (0, 0, 1)X$	$\mathbf{d}(\mathbf{k}) = (1, i, 0)X$
<hr/>		
<i>D</i> _{2h}	Gap function with strong SOC	
A ₁	$\mathbf{d}(\mathbf{k}) = (AX, BY, CZ)$	
B ₁	$\mathbf{d}(\mathbf{k}) = (AY, BX, CXYZ)$	
B ₂	$\mathbf{d}(\mathbf{k}) = (AZ, BXYZ, CX)$	
B ₃	$\mathbf{d}(\mathbf{k}) = (AXYZ, BZ, CY)$	

where the i th index denotes the sample and background contributions, respectively, A_i is the initial asymmetry, σ_i is the Gaussian relaxation rate and ν_i is the muon spin precessional frequency. The background term comes from those muons which were implanted into the silver sample holder and therefore this oscillating term has no depolarisation, i.e. $\sigma_2 = 0.0 \mu\text{s}^{-1}$, as silver has a negligible nuclear moment. Figure 2 shows a typical spectrum for LaNiGa₂ with an applied field of 40 mT at 50 mK after being FC.

As the muon spin rotation arising from the field distributions associated with the flux line lattice is independent of that arising from the nuclear moments we can write $\sigma_1^2 = \sigma_{\text{sc}}^2 + \sigma_n^2$. σ_n is assumed to be constant in this temperature region, and is determined from measurements just above T_c . Each data point was collected after field cooling the sample from above T_c . The field dependence of σ_{sc} (in μs) is related to the superconducting penetration depth λ (in nm) and coherence length ξ via the relation

$$\sigma_{\text{sc}} = 4.83 \times 10^4 (1 - b) [1 + 1.21(1 - \sqrt{b})^3] \lambda^{-2} \quad (2)$$

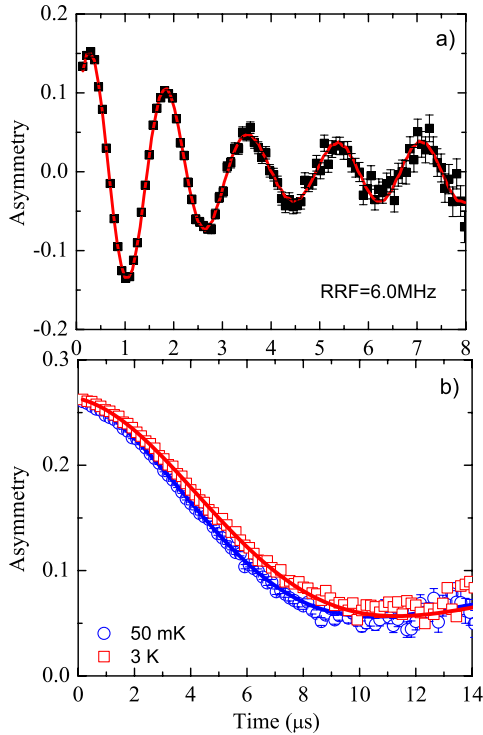


FIG. 2 (color online). The upper graph is a typical muon asymmetry spectra in LaNiGa₂ taken in a transverse field of 40 mT at 0.05 K (shown in the rotating reference frame (RRF) of 6.0 MHz). The line is a fit to the data using Eqn. (1). For clarity, only one of the two virtual detectors have been shown. The lower graph is the zero field μSR spectra for LaNiGa₂. The blue symbols are the data collected at 56 mK and the red symbols are the data collected at 3.0 K. The lines are a least squares fit to the data.

where $b = B/B_{C2}$ is the ratio of applied field to upper critical field. From this we have determined λ and B_{C2} and hence ξ to be 350(10) nm, 410(3) mT and 28(3) nm respectively (see Fig. 3). This shows that LaNiGa₂ is a type II superconductor, with a superconducting electron density and effective superelectron mass of $9 \times 10^{26} \text{ m}^{-3}$ and $3.9m_e$, respectively. More details on these calculations can be found in Ref. [32]. Now let us consider the longitudinal μSR data. The absence of a precessional signal in the μSR spectra at all temperatures confirms that there are no spontaneous coherent internal magnetic fields associated with long range magnetic order in LaNiGa₂ at any temperature. In the absence of atomic moments muon spin relaxation is expected to arise entirely from the local fields associated with the nuclear moments. These nuclear spins are static, on the time scale of the muon precession, and are randomly orientated. The depolarisation function, $G_z(t)$, can be described by the Kubo-Toyabe function [33]

$$G_z^{\text{KT}}(t) = \left(\frac{1}{3} + \frac{2}{3}(1 - \sigma^2 t^2) \exp\left(-\frac{\sigma^2 t^2}{2}\right) \right), \quad (3)$$

where σ/γ_μ is the local field distribution width and $\gamma_\mu = 2\pi \times 135.5 \text{ MHz T}^{-1}$ is the muon gyromagnetic ratio. The spectra that we observed for LaNiGa₂ are well described by the function

$$G_z(t) = A_0 G_z^{\text{KT}}(t) \exp(-\Lambda t) + A_{\text{bckgrd}}, \quad (4)$$

where A_0 is the initial asymmetry, A_{bckgrd} is the background, and Λ is the electronic relaxation rate (see Fig. 2). It is assumed that the exponential factor involving Λ arises from electronic moments which afford an entirely independent muon spin relaxation channel in real time. The only parameter that shows any temperature dependence is σ , which increases rapidly with decreasing temperature below T_c (see Fig. 4). We interpret this increase in σ as a signature of a coherent internal field with a very low frequency as discussed by Aoki *et al.* [9] for PrOs₄Sb₁₂.

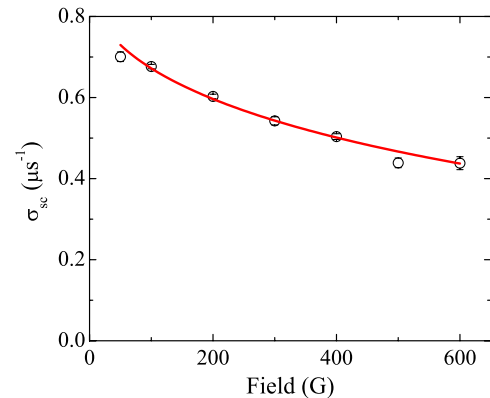


FIG. 3 (color online). The field dependence of σ at 50 mK, after being field cooled. The line is a fit to the data using Eqn. (2).

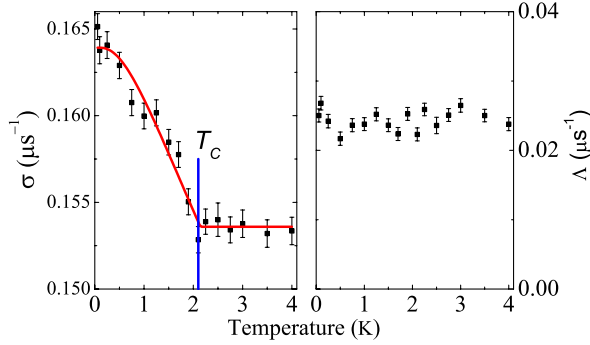


FIG. 4 (color online). The left graph shows the temperature dependence of σ , for LaNiGa₂ in zero-field, which clearly shows the spontaneous fields appearing at $T_c = 2.1$ K (shown as the vertical line). The line is fit to the data using an approximation [34] to the BCS order parameter for σ_e . The right graph shows the temperature dependence of the electronic relaxation rate, Λ , for LaNiGa₂ in zero-field, which shows no temperature dependence.

This increase in σ has been modelled, assuming that there are uncorrelated, by $\sigma(T)^2 = \sigma_n^2 + \sigma_e(T)^2$, where σ_n and σ_e are the nuclear and electronic contributions respectively. The temperature dependence of σ_e agrees with the BCS order parameter (see Fig. 4).

Let us now discuss the implications of this result for the pairing symmetry. The group theoretical analysis for the D_{2h} point group of this system has already been investigated [4]. For the simplest case, where translational symmetry is not broken and SOC does not play a role, this point group has a total of 8 irreducible representations. This leads to 12 possible order parameters, as given in Table I, upper. Of these 12, 8 are unitary and 4 are non-unitary. Only the 4 nonunitary order parameters have a nontrivially complex order parameter that can break TRS. In the case where SOC is large, there are only 4 possible states [see Table I, lower] and none of them break TRS. Therefore, like LaNiC₂, LaNiGa₂ must be a nonunitary triplet superconductor with weak SOC. As we have predicted for LaNiC₂ [7] if the SOC is not zero then a split transition would be expected.

Until the discovery of nonunitary triplet pairing in LaNiC₂ this state had only been confirmed in ferromagnetic superconductors [8]. The additional observation of nonunitary triplet pairing in LaNiGa₂ brings up the question of how a triplet superconductor whose normal state is paramagnetic could favor this state. The usual Landau free energy describing a triplet pairing instability in our system is of the form

$$F = a|\boldsymbol{\eta}|^2 + \frac{b}{2}|\boldsymbol{\eta}|^4 + b'|\boldsymbol{\eta} \times \boldsymbol{\eta}^*|^2 \quad (5)$$

where $\boldsymbol{\eta}$ is the order parameter, which relates to the \mathbf{d} vector through $\mathbf{d}(\mathbf{k}) = \boldsymbol{\eta}\Gamma(\mathbf{k})$ [the possible functional forms of $\Gamma(\mathbf{k})$ are given in Table I, upper]. The triplet

instability takes place when $a = 0$, which determines T_c and is independent of whether pairing is unitary or non-unitary. Below T_c , the second of the quartic terms decides which of the two states is most stable. The criterion for nonunitary triplet pairing is [4]

$$b' < 0. \quad (6)$$

On the other hand, for a paramagnet there must be an additional term coupling $\boldsymbol{\eta}$ to the magnetization \mathbf{m} . On symmetry grounds the simplest form of the free energy that takes this into account is

$$F = a|\boldsymbol{\eta}|^2 + \frac{m^2}{2\chi} + \frac{b}{2}|\boldsymbol{\eta}|^4 + b'|\boldsymbol{\eta} \times \boldsymbol{\eta}^*|^2 + b''\mathbf{m} \cdot (i\boldsymbol{\eta} \times \boldsymbol{\eta}^*). \quad (7)$$

Here, χ is the normal state susceptibility.

For given $\boldsymbol{\eta}$ the last term on the right-hand side of (7) describes an effective magnetic field $\mathbf{h}_{\text{eff}} = -b''(i\boldsymbol{\eta} \times \boldsymbol{\eta}^*)$ coupled to \mathbf{m} . This field vanishes for unitary triplet pairing, but in the nonunitary case it induces a magnetization

$$\mathbf{m} = -\chi b''(i\boldsymbol{\eta} \times \boldsymbol{\eta}^*). \quad (8)$$

Below T_c , $\boldsymbol{\eta} \sim (T_c - T)^{1/2}$ whence $m \sim T_c - T$. This subdominant order parameter lowers the energy of the non-unitary state compared to the unitary one. Indeed substituting (8) into (7) we recover the simpler expression (5) but with the b' coefficient replaced with $b' - b''^2\chi/2$. The condition (6) then becomes

$$b' - b''^2\chi/2 < 0. \quad (9)$$

For a paramagnet, the second term on the left hand side is always negative, favoring nonunitary triplet pairing states. This effect would be expected to be strongest in proximity to a Stoner instability. We note that in superconducting ferromagnets [8] the same coupling term exists and stabilizes nonunitary triplet pairing states by increasing their T_c relative to unitary states.

In conclusion, zero field and transverse field μSR experiments have been carried out on LaNiGa₂. The zero field measurements show a spontaneous field appearing at the superconducting transition temperature. This provides convincing evidence that time reversal symmetry is broken in the superconducting state of LaNiGa₂. Symmetry analysis implies nonunitary triplet pairing, in close analogy with the noncentrosymmetric superconductor LaNiC₂. We propose that these materials could represent a new class of superconductors, where a triplet superconducting instability of a paramagnetic state gives rise to nonunitary pairing through a generic coupling to the magnetization.

This work was supported by EPSRC and STFC (U.K.). J.Q. gratefully acknowledges funding from HEFCE and STFC through the South-East Physics network (SEPnet).

- [1] J. Bardeen, L. N. Cooper, and J. R. Schrieffer, *Phys. Rev.* **108**, 1175 (1957).
- [2] M. Sgrist and K. Ueda, *Rev. Mod. Phys.* **63**, 239 (1991).
- [3] D. M. Lee, *Rev. Mod. Phys.* **69**, 645 (1997).
- [4] J. F. Annett, *Adv. Phys.* **39**, 83 (1990).
- [5] A. P. Mackenzie and Y. Maeno, *Rev. Mod. Phys.* **75**, 657 (2003).
- [6] A. D. Hillier, J. Quintanilla, and R. Cywinski, *Phys. Rev. Lett.* **102**, 117007 (2009).
- [7] J. Quintanilla, A. D. Hillier, J. F. Annett, and R. Cywinski, *Phys. Rev. B* **82**, 174511 (2010).
- [8] A. de Visser, in *Encyclopedia of Materials: Science and Technology* (Elsevier, Oxford, 2010).
- [9] Y. Aoki, A. Tsuchiya, T. Kanayama, S. R. Saha, H. Sugawara, H. Sato, W. Higemoto, A. Koda, K. Ohishi, K. Nishiyama *et al.*, *Phys. Rev. Lett.* **91**, 067003 (2003).
- [10] G. M. Luke, Y. Fudamoto, K. M. Kojima, M. I. Larkin, J. Merrin, B. Nachumi, Y. J. Uemura, Y. Maeno, Z. Q. Mao, Y. Mori *et al.*, *Nature (London)* **394**, 558 (1998).
- [11] J. Xia, Y. Maeno, P. T. Beyersdorf, M. M. Fejer, and A. Kapitulnik, *Phys. Rev. Lett.* **97**, 167002 (2006).
- [12] G. M. Luke, A. Keren, L. P. Le, W. D. Wu, Y. J. Uemura, D. A. Bonn, L. Taillefer, and J. D. Garrett, *Phys. Rev. Lett.* **71**, 1466 (1993).
- [13] P. D. de Reotier, A. Huxley, A. Yaouanc, J. Flouquet, P. Bonville, P. Impert, P. Pari, P. C. M. Gubbens, and A. M. Mulders, *Phys. Lett. A* **205**, 239 (1995).
- [14] W. Higemoto, K. Satoh, N. Nishida, A. Koda, K. Nagamine, Y. Haga, E. Yamamoto, N. Kimura, and Y. Onuki, *Physica (Amsterdam)* **281B–282B**, 984 (2000).
- [15] R. H. Heffner, J. L. Smith, J. O. Willis, P. Birrer, C. Baines, F. N. Gyax, B. Hitti, E. Lippelt, H. R. Ott, A. Schenck *et al.*, *Phys. Rev. Lett.* **65**, 2816 (1990).
- [16] A. Maisuradze, W. Schnelle, R. Khasanov, R. Gumeniuk, M. Nicklas, H. Rosner, A. Leithe-Jasper, Y. Grin, A. Amato, and P. Thalmeier, *Phys. Rev. B* **82**, 024524 (2010).
- [17] L. Shu, W. H. Y. Aoki, A. D. Hillier, K. Ohishi, K. Ishida, R. Kadono, A. Koda, O. O. Bernal, D. E. MacLaughlin, Y. Tunashima *et al.*, *Phys. Rev. B* **83**, 100504(R) (2011).
- [18] D. T. Adroja, A. D. Hillier, J. G. Park, E. A. Goremychkin, K. A. McEwen, N. Takeda, R. Osborn, B. D. Rainford, and R. M. Ibberson, *Phys. Rev. B* **72**, 184503 (2005).
- [19] V. Anand, A. D. Hillier, D. T. Adroja, A. M. Strydom, H. Michor, K. A. McEwen, and B. D. Rainford, *Phys. Rev. B* **83**, 064522 (2011).
- [20] V. H. Tran, A. D. Hillier, and D. T. Adroja, *J. Phys. Condens. Matter* **22**, 505701 (2010).
- [21] A. D. Hillier, N. Parzyk, and D. M. Paul (to be published).
- [22] V. P. Mineev and K. K. Samokhin, *Introduction to Unconventional Superconductivity* (Gordon and Breach, New York, 1999).
- [23] I. Bonalde, R. L. Ribeiro, K. J. Syu, H. H. Sung, and W. H. Lee, *New J. Phys.* **13**, 123022 (2011).
- [24] N. L. Zeng and W. H. Lee, *Phys. Rev. B* **66**, 092503 (2002).
- [25] The authors of Ref. [24] have determined a higher value of $\Delta C/\gamma T_c$ by using a 10%–90% definition of T_c .
- [26] S. Nishizaki, Y. Maeno, and Z. Mao, *J. Phys. Soc. Jpn.* **69**, 572 (2000).
- [27] V. K. Pecharsky, L. L. Miller, and J. K. A. Gschneider, *Phys. Rev. B* **58**, 497 (1998).
- [28] R. Gumeniuk, W. Schnelle, H. Rosner, M. Nicklas, A. Leithe-Jasper, and Y. Grin, *Phys. Rev. Lett.* **100**, 017002 (2008).
- [29] S. L. Lee, S. H. Kilcoyne, and R. Cywinski, *Muon Science: Muons in Physics, Chemistry and Materials* (SUSSP Publications and IOP Publishing, Bristol, 1999).
- [30] A. Yaouanc and P. D. de Reotier, *Muon Spin Rotation, Relaxation, and Resonance* (Oxford University Press, New York, 2011).
- [31] A. Schenck, *Muon Spin Rotation Spectroscopy Principles and Applications in Solid State Physics* (Taylor and Francis, London, 1985).
- [32] A. D. Hillier and R. Cywinski, *Appl. Magn. Reson.* **13**, 95 (1997).
- [33] R. S. Hayano, Y. J. Uemura, J. Imazato, N. Nishida, T. Yamazaki, and R. Kubo, *Phys. Rev. B* **20**, 850 (1979).
- [34] A. Carrington and F. Manzano, *Physica (Amsterdam)* **385C**, 205 (2003).